JOURNAL OF MATERIALS SCIENCE 25 (1990) 4965–4971

The dielectric properties of aluminium nitride substrates for microelectronics packaging

J. S. THORP*, D. EVANS‡, M. AL-NAIEF*, M. AKHTARUZZAMAN‡
*School of Engineering and Applied Science and
‡Department of Physics, University of Durham, Durham, DH1 3LE, UK

The dielectric behaviour of sintered polycrystalline aluminium nitride substrates has been examined over the frequency range 500 Hz to 10 MHz and correlated with composition and microstructure. For pure, white AlN at 20° C both the permittivity (ε') and dielectric loss (ε'') are frequency independent giving $\varepsilon' = 9.2 \pm 0.05$ and $\tan \delta = (2.1 \pm 0.1) \times 10^{-3}$. The permittivity is less than for pure alumina substrates ($\varepsilon' = 10.2$) but $\tan \delta$ compares favourably, with that (1.4×10^{-3}) of alumina, which though used more widely has a thermal conductivity some eight times less than that of AlN. The addition of impurities, particularly iron, to give opaque black AlN causes large, frequency dependent increases in ε''; at 500 Hz the loss is seven times that of pure white AlN and is two times greater above 100 kHz. The temperature coefficient of permittivity $[(\varepsilon' - 1)(\varepsilon' + 2)]^{-1}[\partial\varepsilon/\partial T]_p$ between −180 and +180° C for pure white AlN is $1.05 \times 10^{-5}\,K^{-1}$ which is similar to the value of $9 \times 10^{-6}\,K^{-1}$ for pure Al_2O_3. For impure black AlN the coefficient below 20° C is the same but above 20° C there is a rapid, non-linear increase of ε' with temperature. Below 180° C for pure white AlN and 20° C for impure black AlN the values of temperature coefficient are frequency independent at least up to 200 kHz.

1. Introduction

There is currently considerable interest in dielectric materials which are suitable for substrates in microelectronic packaging applications. The choice of a substrate has to balance several important and sometimes conflicting physical properties. Thus, while the electrical characteristics of low dielectric loss and medium range permittivity are needed, other factors such as thermal expansion coefficient matching, mechanical strength, and not least, thermal conductivity must also be considered. For packages utilizing silicon chip technology current contenders include alumina, glass and glass ceramics. In general these can provide adequate dielectric properties, giving at 1 kHz permittivities in the range $4 < \varepsilon' < 10$ with values of loss, expressed as $\tan \delta$, of between about 10^{-3} and 10^{-4} at room temperature. For high power packages, however, these three types of substrate have a common disadvantage in that they all possess low thermal conductivities which limit the power dissipations attainable. Both beryllia and aluminium nitride have been suggested as alternatives since they have much greater thermal conductivities than alumina; some comparative data [1] are given in Table I. Toxicity problems are associated with the fabrication of beryllia components and thus attention has been focused on aluminium nitride.

A systematic study of dielectric properties of commercially available substrate materials is currently being carried out in this laboratory. An important feature of this study is the simultaneous characterization of the impurities in, and structure of, the materials being measured.

The data obtained on alumina based substrate materials have already been published [2]. In the present work we have made dielectric measurements on solid sintered polycrystalline aluminium nitride substrates. These were obtained as commercially available substrates from different sources and were provided in thin sheet form, one group of which appeared white in colour and the other black. A number of characterization measurements were made in order to assess the purity and microstructure of the sheet materials; these measurements were also made on the powder which was the starting materials for the black substrate. The dielectric measurements covered two aspects; room temperature measurements of permittivity (ε') and dielectric (ε'') were made over the frequency range 500 Hz to 10 MHz using bridge and Q-meter techniques similar to those used in previous work [3], and the variation of permittivity at a number of frequencies was examined over the temperature range −188° to 400° C using methods developed previously [4, 5]. These measurements required the preparation of samples in the form of thin slices (10 mm × 10 mm × 0.5 mm) with surfaces made flat and parallel by lapping and polishing techniques which gave the surface flatness to within 0.25 μm.

2. Structural and chemical characterization

2.1. XRD, XRF and EDAX methods

Scanning electron microscopy (SEM) was used in order to ascertain the general features and grain sizes of the two sintered materials. Some results are shown in Figs 1a and b. For the white material the average

0022–2461/90 $03.00 + .12

TABLE I Thermal conductivity data

Material	Conductivity ($W m^{-1} K^{-1}$)	Material	Conductivity ($W m^{-1} K^{-1}$)
Si	95–100	BeO	350
GaAs	80	Y_2O_3	40
SiC	120	Al_2O_3	25
Diamond	1800	SiO_2	12
AlN	~200	MgO	24

grain size is between 4 and 6 μm and there appeared to be some smaller grains (about 0.25 μm in diameter) randomly dispersed throughout the materials. By contrast the black material, Fig. 1b, reveals a much coarser texture, many grains being as large as about 12 μm. In addition there is evidence for quite large (2 to 10 μm) flakes of different materials but there is a markedly smaller density of the small grains present in Fig. 1a.

X-ray diffractometry was used to ascertain crystallographic details of the two substrates. Aluminium nitride is hexagonal with unit cell dimensions a = 0.3220 nm [6]. The experimental interplanar spacings obtained are listed in Table II which gives for comparison the ASTM data. It can be seen that for the white substrate all the lines expected were observed, that there was very close agreement of the observed d-values with the ASTM listing and that there were no additional lines in the XRD spectrum. This suggested that this material was substantially single phase, high purity aluminium nitride. By contrast the black material showed all the expected hexagonal AlN lines together with four clearly identifiable additional lines occurring at d-values of 0.1241, 0.0970, 0.0912 and 0.0896 nm. To elucidate further the nature of the impurities causing

TABLE II X-ray diffractometer analysis of AlN substrate materials

ASTM data*		AlN (W)		AlN (B)	
d (nm)	hkl	d (nm)	hkl	d (nm)	hkl
0.270	100	0.2693	100	0.2685	100
0.249	002	0.2483	002	0.2475	100
0.2372	101	0.2366	101	0.2354	101
0.1829	102	0.1827	102	0.1826	102
0.1557	110	0.1552	110	0.1553	110
0.1414	103	0.1413	103	0.1411	103
0.1348	200	0.1342	200	0.1343	200
0.1320	112	0.1319	112	0.1318	112
0.1301	201	0.1201	201	0.1298	201
–	–	–	–	0.12410	Impurity
0.1186	202	0.1183	202	0.1181	202
0.1047	203	0.1044	203	0.1046	203
0.0997	211	0.0997	211	0.0997	211
–	–	–	–	0.0970	Impurity
0.0941	212	0.09414	212	0.09414	212
0.0934	105	0.0932	105	0.0930	105
–	–	–	–	0.09128	Impurity
–	–	–	–	0.08969	Impurity
0.0868	213	0.0888	214	0.0887	213

*American Society for Testing Materials.

these additional lines X-ray fluorescent (XRD) and energy dispersive (EDAX) analyses were also made. Both these techniques yield elemental composition. The XRF data are summarized in Table III which refers to impurity level constituents for the white substrate W, two separate samples of the black substrate (B1 and B2) and the starting powder (B3) from which B1 and B2 were made and which was itself a dark grey colour. The major impurity in W is titanium; there are lesser amounts of chromium and calcium, a small level of iron and no detectable silicon. By contrast the black substrates contain very much higher iron contents, more silicon, some zinc but no calcium; it appears that most of the iron is carried over from that present in the starting powder, but that some of the other impurities may be picked up during the substrate fabrication stages. The EDAX analyses, Fig. 2, confirmed that

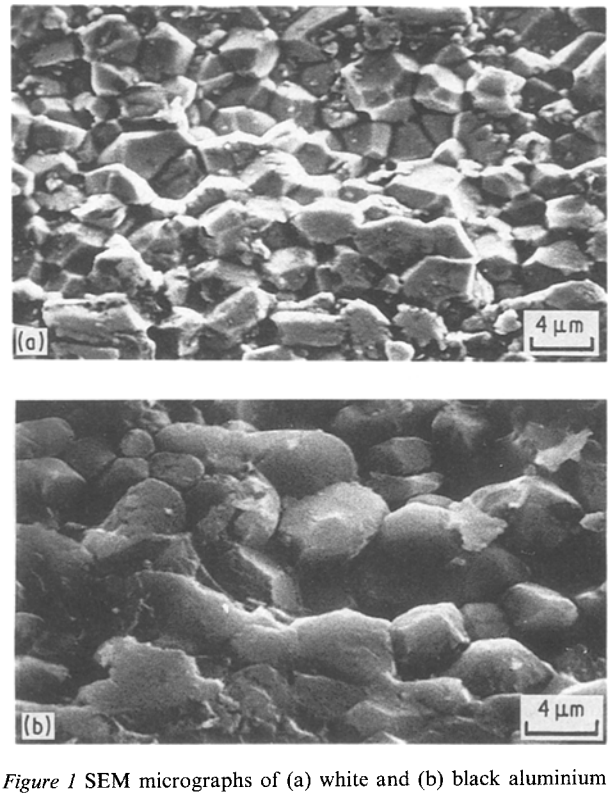

Figure 1 SEM micrographs of (a) white and (b) black aluminium nitride substrates.

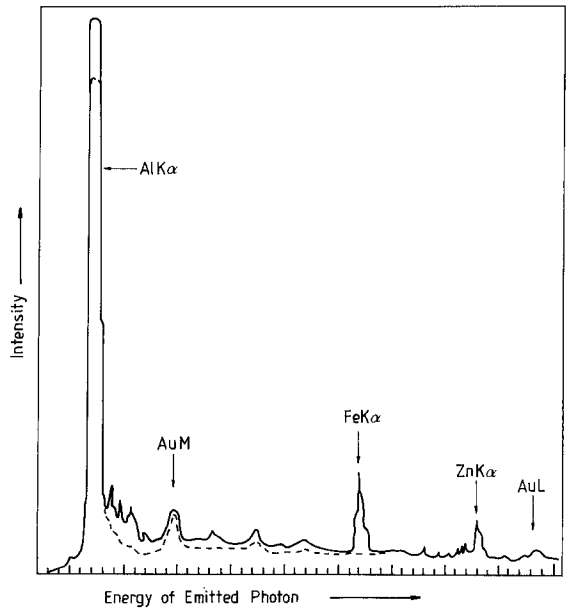

Figure 2 EDAX spectrum of black AlN substrate (full line, region 1; dotted line, region 2; electron beam diameter 0.5 μm).

TABLE III X-ray fluorescent analysis of AlN samples (in p.p.m.)

Major impurity	Substrate			Powder B3
	(W)	(B1)	(B2)	
Fe	30	2600	1400	2000
Si	–	210	40	600
Cr	200	79	107	–
Zn	–	600	–	140
Ti	600	330	200	–
Ca	300	–	–	–

TABLE IV Room temperature ferromagnetic resonance data for some elements and oxides compared with observed data for black AlN and for substitutional (paramagnetic) iron

Elements and compounds	Linewidth (mT)	g Factor	Reference
Fe	16.0	2.004	[7, 8]
Ni	13.0	2.22	[9, 10]
Co	15.5	2.021	[9]
Fe_3O_4	250.0	2.016	[6]
Black $Al(B_2)$	296	2.011	[6]
Iron doped alumina, Fe^{3+}/Al_2O_3 powder (1000 p.p.m.)	2.17	2.002	[6]

presence of iron as a major impurity and also gave clear evidence that the iron was not uniformly distributed throughout the AlN matrix. (In Fig. 2 the AuM and AuL spectra arise from a thin layer of gold evaporated over the sample to avoid charging effects and do not represent an impurity.)

2.2. Magnetic techniques

Magnetic measurements were also used to assist characterization of the iron in the black aluminium nitride. Magnetic resonance at 9 GHz and magnetic susceptibility measurements were employed and the applicability of these to ferromagnetic impurity assessment has been discussed by Al-Naief [7]. At room temperature the white substrate gave no detectable magnetic resonance signals indicating (in conformity with earlier XRD and XRF data) that paramagnetic or ferromagnetic species, if present at all, were at very low concentrations. All the black samples, however, gave strong single resonance features having a broad line with $g = 2.011$ and width between 200 and 300 mT. An example is shown in Fig. 3. From general experience it is likely that the signal is of ferromagnetic or ferrimagnetic origin, either due to elemental iron or to an iron compound possibly a ferrimagnetic oxide of iron, e.g. Fe_3O_4. This latter would also be compatible with both the XRF and EDAX scans since in neither is oxygen detectable. Some FMR resonance data given in Table IV show that none of the listed elements has a linewidth at all comparable with that observed. For iron oxide however, the linewidth, (250 mT) is quite comparable with that found in the black AlN and its g value is also close to 2.011. For substitutional iron, i.e. Fe^{3+}/AlN, the ESR linewidth would be expected to be of the same order as that found in iron doped alumina (Fe^{3+}/Al_2O_3); this is only about 3 mT for an iron concentration of about 1000 p.p.m., which represents the maximum level of iron which would be accommodated in the lattice.

Measurements of magnetic susceptibility (χ) and Curie temperature (θ_c), were made using Gouy balance techniques [12]. The room temperature variation of force against field gave at all fields a positive gradient, though there was a marked departure from linearity at the higher fields indicative of a non-paramagnetic component [13]. In the low field region the volume susceptibility was found to be $\chi = +21.5\,J\,T^{-2}\,m^{-3}$, proving that the sample was certainly not diamagnetic. It should be noted here that pure AlN is diamagnetic [14] and the experimental result is thus consistent with the presence of ferri- or ferromagnetic impurities. The Curie temperature was determined by observing the change of force with temperature at a fixed magnetic field. As a test of the technique, measurements were first made with nickel powder; these are shown in Fig. 4a and give $\theta_c = (366 \pm 10)^\circ C$ in good agreement with the value (355° C) quoted in the literature [14]. For the black AlN, Fig. 4b, the force curve approaches zero in a more complex manner than is the case for nickel comparison. The Curie temperature for iron is 770° C [15] and Fig. 4b shows that the magnetisation has become small at that temperature. For the ferrite Fe_3O_4, however, the Curie temperature is 575° C and one could remark on a drop in magnetization in that region. One can only conclude that the iron is probably present both as an element and in compound form, the combination exhibiting a complicated behaviour of magnetization with temperature. Indeed the shallow

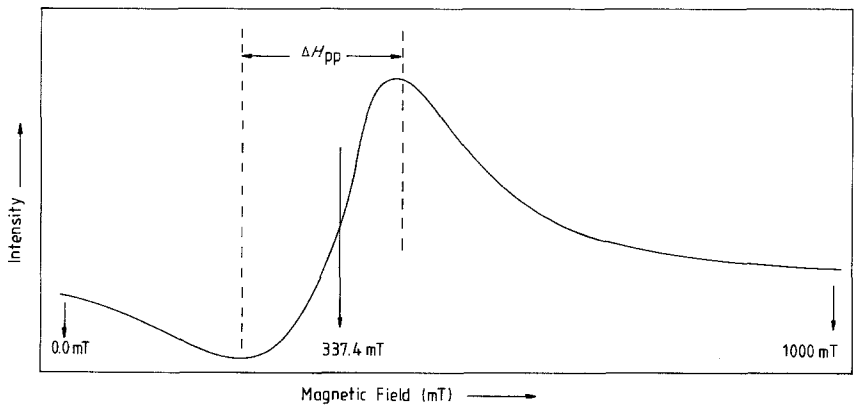

Figure 3 EPR spectrum of black AlN substrate; 9.50 GHz, 293 K.

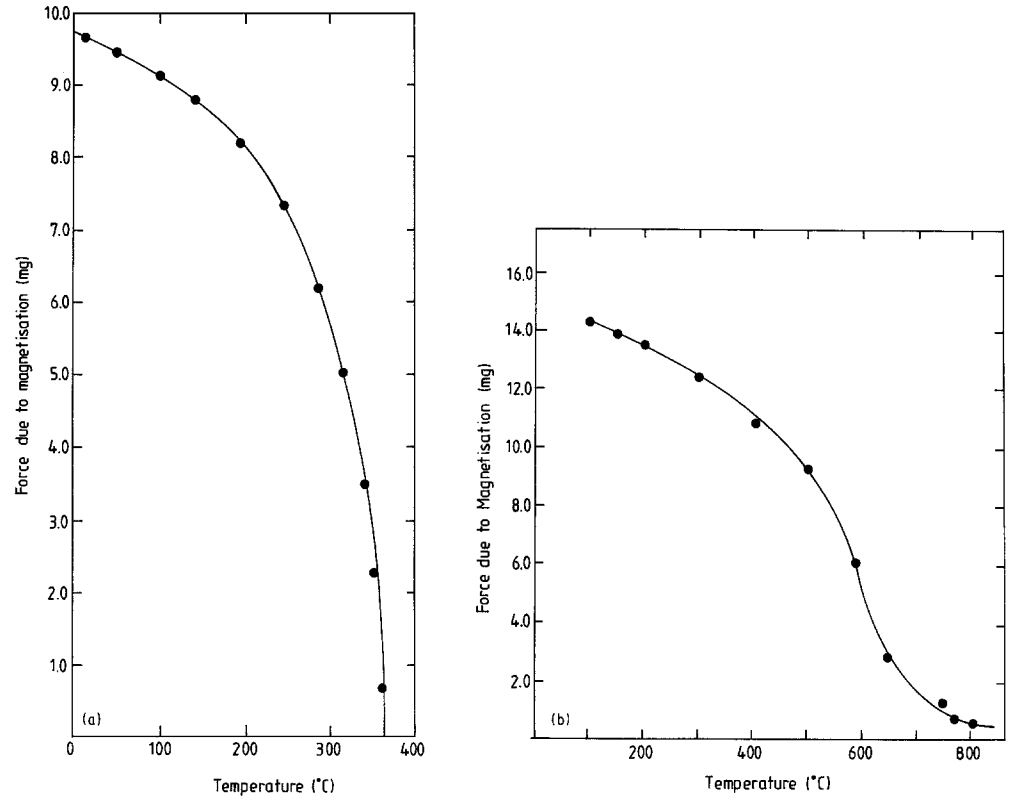

Figure 4 (a) Force–temperature variation for nickel powder. (b) Force–temperature variation for black AlN.

slope of the curve in Fig. 4b above 650° C (c.f. Fig. 4a) could be due to the presence of several magnetic phases with different values of θ_c.

3. Dielectric properties

3.1. Room temperature results and discussion

Since both the white and the black AlN substrates were sintered polycrystalline materials, they were not fully dense, and a small correction for porosity, p, was necessary in order to convert the experimentally measured permittivity, ε_p', and dielectric loss ε_p'' to the corresponding values, ε_s' and ε_s'', respectively, of the equivalent solid. For permittivity, the relation

$$(\varepsilon_p')^{1/3} - 1 = p[(\varepsilon_s')^{1/3} - 1]$$

given by Looyenga [16] for spherical particles was used. For dielectric loss, since the criterion that $\varepsilon''/\varepsilon' \ll 1$ was certainly satisfied, the correction was made using the expression [17].

$$\varepsilon_s'' = \frac{\varepsilon_p''}{p}\left(\frac{\varepsilon_s'}{\varepsilon_p}\right)^{2/3}$$

This is also derived for spherical particles. For both the white and black AlN the densities were about 80% of those of the crystalline solid and the corrections amounted to some 10%.

The room temperature variations of permittivity and dielectric loss with frequency are shown in Figs 5 and 6. Over the frequency range 500 Hz to 10 MHz, the permittivities are almost entirely frequency independent. Fig. 5a shows that $\varepsilon_s' = 9.2$ for the white AlN which is rather smaller than the value of $\varepsilon_s' = 10.2$ for the pure Al_2O_3 [2]. Fig. 5b shows that the

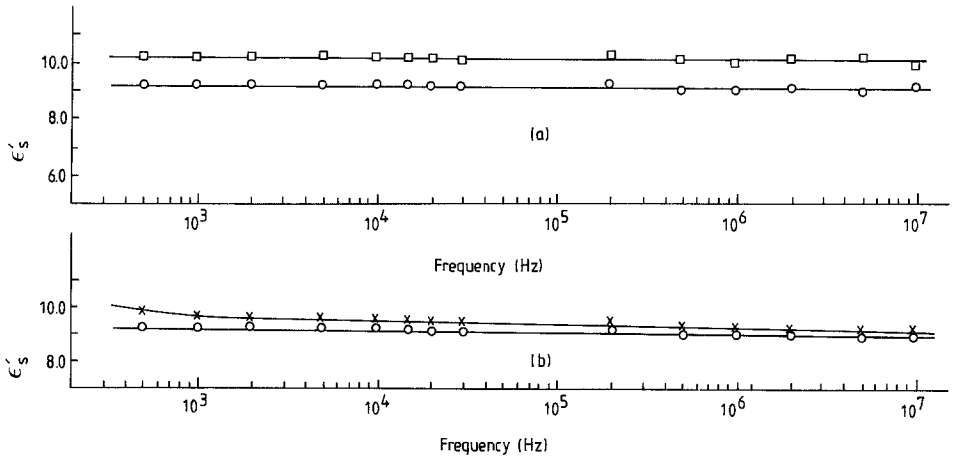

Figure 5 Comparison of permittivity against frequency variations for (a) pure polycrystalline AlN (○) and pure polycrystalline Al_2O_3 (□) and (b) pure polycrystalline AlN (○) and black polycrystalline AlN (×).

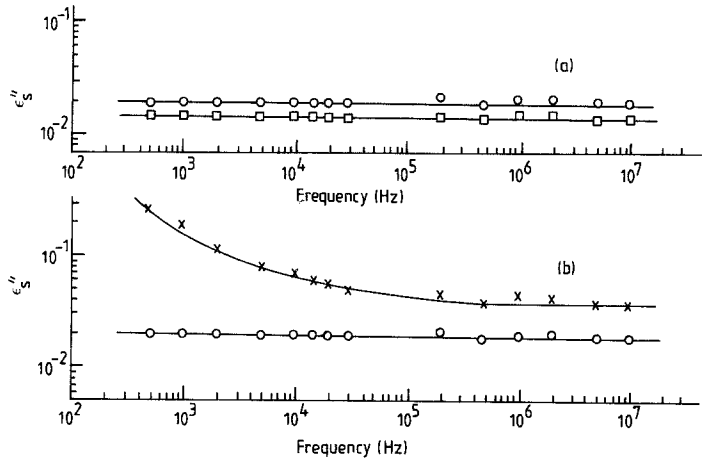

Figure 6 Comparison of dielectric loss against frequency variations for (a) pure polycrystalline AlN (○) with pure polycrystalline Al_2O_3 (□) and (b) pure polycrystalline AlN (○) with black polycrystalline AlN (×).

permittivity of the black material is higher than that of the white, the difference being noticeably larger at the low frequency end of the range. The dielectric loss data are shown in Fig. 6, where it is seen that, as with Al_2O_3, ε_s'' is practically frequency independent though somewhat higher than for alumina in the case of the white nitride substrate while the black material shows higher values of ε_s'' which have large variations below 100 kHz. Thus for the white AlN the tan δ value is about 2.17×10^{-3} over the whole frequency range and compares quite favourably with the value of 1.47×10^{-3} for pure polycrystalline alumina, while even at frequencies above 100 kHz the dielectric loss for the black AlN is about twice that of the white nitride. Below 100 kHz ε_s'' for black AlN rapidly becomes greater, being nearly a factor of seven times the value for the white substrate at 500 Hz. This is typical of increased polarization due to impurities at grain boundaries and defects in structure, which is most pronounced at low frequency.

There are some reports in the literature of the dielectric properties of both single crystal and thin film aluminium nitride [18]. Single crystals of aluminium nitride have been grown for some years by methods which mostly involve subliming AlN in pure nitrogen atmospheres at temperatures approaching 2000° C [19]. These crystals have been sufficiently well formed to enable the habit and crystallographic characteristics to be determined but, since they mostly had dimensions not exceeding a few millimetres, were not suitable for conventional a.c. bridge dielectric measurement techniques. Collins, Lightowlers and Dean [20], however, observed the lattice vibration spectra of single crystal aluminium nitride by recording the optical reflectivity and transmission spectra in the wavelength range 2 to 30 μm. From these measurements they found that the optical refractive index was 2.2 and quoted a value of ε_∞' of 4.84. They deduced a value of the low frequency permittivity of $\varepsilon' = 9.14$, which agrees very well with our value of 9.2 obtained for the white substrate sample. A comparison with data on aluminium nitride film can also be made using one of the recent papers published by Chu and Kelm [21]. These authors measured the dielectric properties of aluminium nitride films by making capacitance measurements using a bridge operating at frequencies up to 5×10^5 Hz. For films prepared at temperatures between 800 and 1000° C ε' was found to be 11.5, whereas for films prepared at the higher temperature of 1100° C the permittivity was considerably lower, being about 8.1; Chu and Kelm also reported that ε' was independent of frequency up to 5×10^5 Hz but gave no data on dielectric loss.

The low frequency data presented here suggest fairly convincingly for the white AlN that application of the Universal law [22] is appropriate. Fitting the AlN data of Figs 6a and 7a to the expressions (ω is frequency)

$$(\varepsilon_s' - \varepsilon_\infty') \propto \omega^{n-1}$$

and

$$\varepsilon_s'' \propto \omega^{n-1}$$

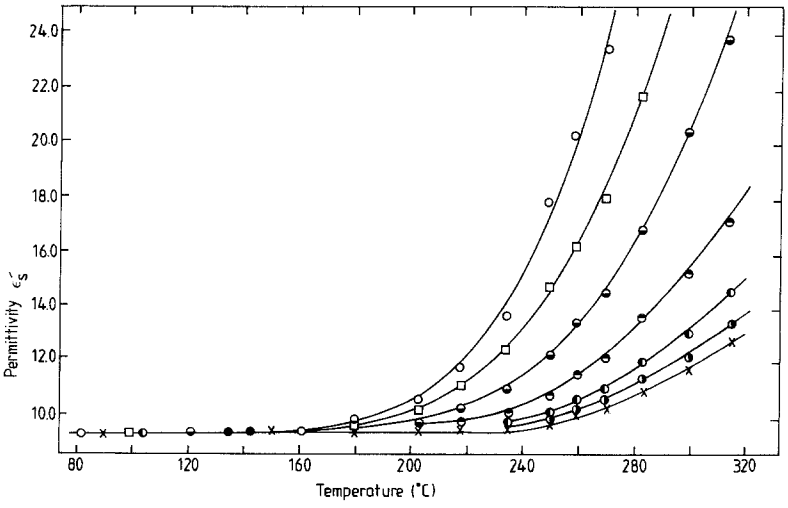

Figure 7 Temperature variation of ε_s' for pure polycrystalline AlN; high temperature range. (500 Hz (○), 1 kHz (□), 2 kHz (◒), 5 kHz (◓), 10 kHz (◐), 15 kHz (◑), 20 kHz (×).)

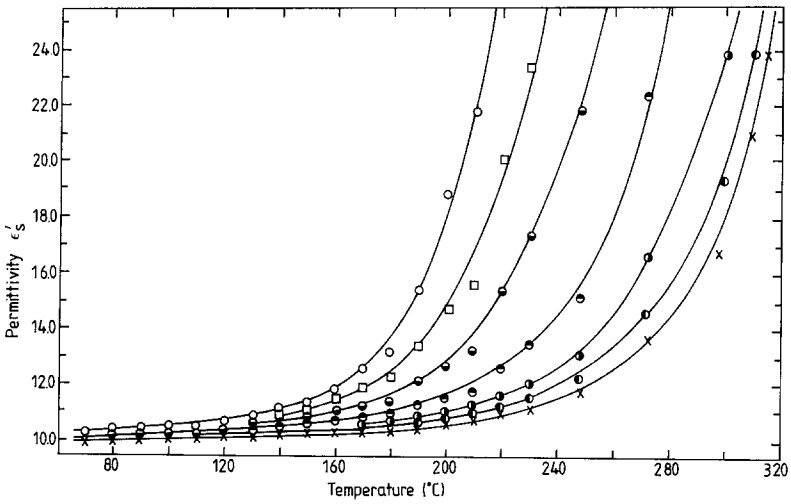

Figure 8 Temperature variation of ε_s' for black AlN; high temperature range. (500 Hz (○), 1 kHz (□), 2 kHz (◒), 5 kHz (◓), 10 kHz (◐), 15 kHz (◑), 20 kHz (×).)

and using $\varepsilon_\infty' = 4.84$ from [20], gives values of the exponent n of 0.97 ± 0.03 (for pure AlN) from the permittivity–frequency variation and 0.96 ± 0.04 from the dielectric loss–frequency variation.

Extrapolation or the ε_s' relation yields a predicted value of permittivity of 8.8 ± 0.1 at 10^{10} Hz for pure polycrystalline aluminium nitride. This agrees well with that obtained by Taylor and Lenie [22] who reported that for hot-pressed aluminum nitride which was about 96% pure and whose density was 98% of theoretical $\varepsilon' = 8.5$ also at the frequency of 10^{10} Hz. This agreement suggests that the Universal law behaviour does hold for frequencies up to the microwave region. If, however, the extrapolation were to be taken further the predicted value at optical frequencies would be about 8.5 which is clearly very much in excess of the measured value of 4.84 deduced from the optical refractive index. It is not surprising that the low frequency region has contributions from polarization mechanisms that cannot respond to optical frequencies. It would seem, however, that the contributions to the polarization remain much the same from 0.5 kHz to 10 GHz.

3.2. The temperature dependence of permittivity

Measurements of permittivity as a function of temperature were made in two regions, the first using a furnace covering the temperature range 20 to 350° C and the second utilizing a cryostat operating between −190 and 20° C. The results are shown in Figs 7, 8 and 9. The data for white aluminium nitride in the upper temperatures region, are given in Fig. 7. Between room temperature and about 150° C, there is a smaller linear increase of ε_s' with temperature and the data for all the different frequencies, i.e. 500 Hz to 200 kHz, fall within very close limits. Above 150° C ε_s' begins to increase rapidly giving very non-linear behaviour; it is noticeable that the rate of change $[\delta\varepsilon'/\delta T]_p$ (P = constant pressure), increases progressively as temperature increases and that at a given temperature is larger at lower frequencies than at higher ones. It is also seen that the point at which the change from linear to non-linear behaviour occurs varies with frequency; thus for 500 Hz the changeover occurs near 160° C whereas at 200 kHz, the plot remains linear until nearly 230° C. The corresponding data for the black substrates are shown in Fig. 8. The same general features pertain but it is clear that the linear regions are much reduced in extent. The low temperature data, covering the range from room temperature down to −190° C, are shown in Fig. 9, which gives the results for both the white and black AlN specimens. The graphs show that there is now little variation either with temperature or frequency. Analysis of the data in the linear ranges, i.e. for temperatures ranging from −190 to about 180° C has been undertaken on the basis of the Bosman and Havinga model [23]. The value of the temperature coefficient $[(\varepsilon' - 1)(\varepsilon' + 2)]^{-1}[\delta\varepsilon'/\delta T]_p$ for the white aluminium nitride is about 1.05×10^{-5} K^{-1}. For the black sample the value below room temperature is the same, but above 20° C the non-linearity of the ε' against temperature plot is very marked and the model would

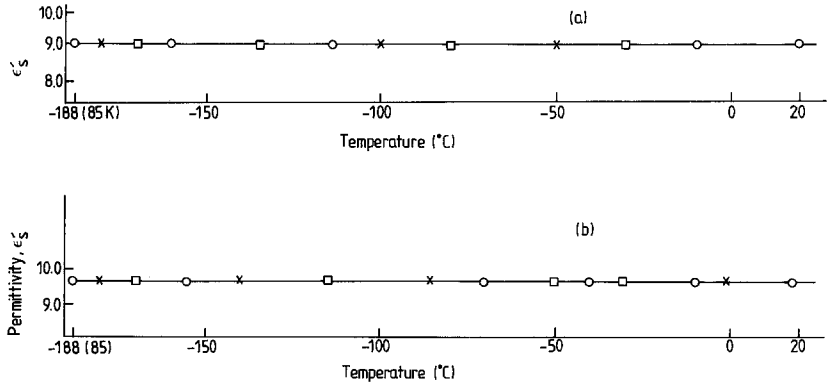

Figure 9 Temperature variation of permittivity for (a) pure polycrystalline aluminium nitride and (b) black aluminium nitride; low temperature region. (1 kHz (○), 10 kHz (□) and 20 kHz (×).)

then not be applicable. Below 180° C for pure AlN and 20° C for black AlN these values of temperature coefficient are frequency independent at least up to 200 kHz.

From the point of view of utilizing aluminium nitride as a substrate material for microelectric packaging applications, it is important to make a comparison of its properties with those of its chief competitor, aluminium oxide. This can be done by utilizing the dielectric data on substrate grade alumina recently measured here [2, 4]. For pure AlN (white) substrates the permittivity is 9.2 at 20° C and 1 kHz compared with 10.2 for pure Al_2O_3 (also a white substrate) under the same conditions; for both materials the permittivity is frequency independent up to at least 1 MHz. The temperature coefficients of permittivity, defined over the linear regions of the ε' against T plots are $1.1 \times 10^{-5} K^{-1}$ for AlN and $9.3 \times 10^{-6} K^{-1}$ for Al_2O_3. It is noticeable, however, that the temperature coefficient remains constant to a significantly higher temperature (260° C) for Al_2O_3 than for AlN (180° C); above these respective temperatures the values of the coefficients increase rapidly. In the case of both alumina and nitride substrates, the addition of impurities to produce black material leads to a degradation of dielectric properties.

4. Conclusions

Commercially available aluminium nitride substrates have been characterized and their dielectric properties measured. It is found that substrates not containing transition metal impurities such as iron and white rather than black in appearance have far superior dielectric properties, the values of permittivity (ε') and loss (ε'') having little variation with frequency possibly up to 10 GHz and temperature below 180° C.

Compared with alumina substrates of similar purity and also white in appearance there is little difference in the value of ε' which is 9.2 for the nitride and 10.2 for the oxide at 20° C and 1 kHz. The nitride has slightly more loss with a value of tan δ of 2.2×10^{-3} compared with 1.47×10^{-3} for alumina. The two types of substrates are good packaging materials as long as they are pure. The commercial introduction of impurities which seem to be mainly iron, in order to produce a black substrate leads to a severe degradation of electrical properties, particularly if temperatures much in excess of 50° C are to be encountered.

Acknowledgements

We wish to express our thanks to the SERC/Alvey High Performance Packaging Consortium through which some of the materials examined were obtained. Two of us (M. Al-Naief and M. Akhtaruzzaman) wish to express our thanks to the King Saud University, Kingdom of Saudi Arabia and to the University of Rajshahi, Bangladesh respectively for the award of a Research Scholarship.

References

1. R. BERMAN, "Thermal Conduction in Solids" (Clarendon, Oxford, 1978).
2. J. S. THORP, M. AKHTARUZZAMAN and D. EVANS, *J. Mater. Sci.*, in press.
3. J. S. THORP and N. E. RAD, *ibid.* **16** (1981) 255.
4. J. S. THORP, M. E. RAD, D. EVANS and C. D. H. WILLIAMS, *ibid.* **21** (1986) 3091.
5. Md. AKHTARUZZAMAN, PhD thesis, University of Durham (1989).
6. F. OTT, *Z. Physik* **22** (1924) 201.
7. M. AL-NAIEF, PhD thesis, University of Durham (1988).
8. S. BHAGAT, L. L. HIRST and J. R. ANDERSON, *J. Appl. Phys.* **37** (1966) 1.
9. B. BLEANEY and K. W. H. STEVENS, *Rep. Prog. Phys.* **18** (1955) 304.
10. S. BHAGAT and P. LUBLITZ, *Phys. Rev. B* **10** (1974) 179.
11. S. BHAGAT, J. R. ANDERSON and N. WU, *Phys. Rev.* **155** (1967) 510.
12. J. S. THORP, A. P. JOHNSON and C. SAVAGE, *J. Mater. Sci. Lett.* **4** (1985) 221.
13. C. D. H. WILLIAMS, S. R. HOON and J. S. THORP, *ibid.* **5** (1986) 832.
14. R. C. WEAST, "Handbook of Chemistry and Physics", 57th edn. (CRC, Cleveland, Ohio, 1976) p. E120.
15. R. M. BOZORTH, "Ferromagnetism" (Van Nostrand, London, 1951).
16. H. LOOYENGA *Physica* **31** (1965) 401.
17. D. C. DUBE, *J. Phys. D.* **3** (1979) 1648.
18. H. D. WIRZKE, *Phys. Status Solidi* **2** (1962) 1109.
19. J. PASTRNAK and L. ROSKOVCOVA, *Phys. Status Solidi* **7** (1964) 331.
20. A. T. COLLINS, E. C. LIGHTOWLERS and P. J. DEAN, *Phys. Rev.* **158** (1967) 833.
21. T. L. CHU and R. W. KELM, *J. Electrochem. Soc.* **122** (1975) 995.
22. K. M. TAYLOR and C. LENIE, *ibid.* **107** (1960) 308.
23. A. J. BOSMAN and E. E. HAVINGA, *Phys. Rev.* **127** (1963) 1593.

Received 11 October
and accepted 19 October 1989